

# Contribution of Two-Boson-Exchange with $\Delta(1232)$ Excitation to Parity-Violating Elastic Electron-Proton Scattering

Keitaro Nagata<sup>1</sup>, Hai Qing Zhou<sup>2</sup>, Chung Wen Kao<sup>1</sup>, and Shin Nan Yang<sup>3,4</sup>

<sup>1</sup>Department of Physics, Chung-Yuan Christian University, Chung-Li 32023, Taiwan

<sup>2</sup>Department of Physics, Southeast University, Nanjing 211189, China

<sup>3</sup>Department of Physics and <sup>4</sup>Center for Theoretical Sciences, National Taiwan University, Taipei 10617, Taiwan

(Dated: September 23, 2021)

We study the leading electroweak corrections in the precision measurement of the strange form factors. Specifically, we calculate the two-boson-exchange (TBE), two-photon-exchange (TPE) plus  $\gamma Z$ -exchange ( $\gamma ZE$ ), corrections with  $\Delta(1232)$  excitation to the parity-violating asymmetry of the elastic electron-proton scattering. The interplay between nucleon and  $\Delta$  contributions is found to depend strongly on the kinematics, as  $\delta_\Delta$  begins as negligible at backward angles but becomes very large and negative and dominant at forward angles, while  $\delta_N$  always stays positive and decreases monotonically with increasing  $\epsilon$ . The total TBE corrections to the extracted values of  $G_E^s + \beta G_M^s$  in recent experiments of HAPPEX and G0 are, depending on kinematics, found to be large and range between 13% to  $-75\%$  but small in the case of A4 experiments.

PACS numbers: 13.40.Ks, 13.60.Fz, 13.88.+e, 14.20.Dh

Recently, parity-violating (PV) elastic electron-proton scattering has been actively pursued [1] in order to probe the strangeness content of the nucleon, one of the most intriguing questions in hadron structure in the last two decades. It is achieved by measuring the parity-violating asymmetry  $A_{PV} = (\sigma_R - \sigma_L)/(\sigma_R + \sigma_L)$ , where  $\sigma_{R(L)}$  is the cross section with a right- (left-) handed electron, in scattering of longitudinally polarized electrons from unpolarized protons. At tree level, parity violation in electron scattering comes from the interference between one-photon-exchange (OPE) and  $Z$ -boson-exchange (ZBE) diagrams as shown, respectively, in Figs. 1(a) and 1(b). The form factors of neutral weak current extracted from  $A_{PV}$  are sensitive to a different linear combination of the three light quark distributions. When combined with proton and neutron electromagnetic form factors and with the use of charge symmetry, the strange electric and magnetic form factors,  $G_E^s$  and  $G_M^s$ , can then be determined [2].

Leading order radiative corrections to  $A_{PV}$ , including the box diagrams Fig. 1(d) and other diagrams, were extensively studied in [3, 4] where the interference between  $\gamma Z$ -exchange ( $\gamma ZE$ ) of Fig. 1(d) with Fig. 1(a), was evaluated within the zero momentum transfer approximation, i.e.,  $Q^2 = 0$ . However, recent studies [5, 6] indicate that the  $\gamma ZE$  correction has a strong  $Q^2$  dependence which could lead to substantial errors in the extracted strange form factors if the results obtained with  $Q^2 = 0$  are used.

In addition, the contribution of the interference of the two-photon-exchange (TPE) process of Fig. 1(c) with diagram of Figs. 1(a) and 1(b) to  $A_{PV}$ , has been calculated in [7] in a parton model using GPDs. It was found that indeed the TPE correction to  $A_{PV}$  can reach several percent in certain kinematics, becoming compa-

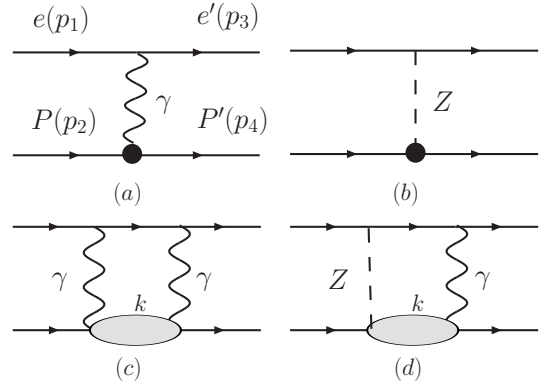


FIG. 1: (a) one-photon-exchange, (b)  $Z$ -boson-exchange, (c) TPE, and (d)  $\gamma Z$ -exchange diagrams for elastic  $ep$  scattering. Corresponding cross-box diagrams are implied.

table in size with existing experimental measurements of strange-quark effects in the proton neutral weak current. The results of the partonic calculation of [7] at large  $Q^2$  have been confirmed by the hadronic calculations of [5, 6].

The calculations of [5, 6] which studied the two-boson-exchange (TBE) corrections to  $A_{PV}$ , namely, the contributions of the interference of the TPE process of Fig. 1(c) with diagram of Figs. 1(a) and 1(b) to  $A_{PV}$ , and that between the  $\gamma ZE$  of Fig. 1(d) with Fig. 1(a), were carried out in a simple hadronic model where the intermediate states are restricted only to elastic intermediate states. Since  $\Delta(1232)$  plays a dominant role in low-energy hadron physics [8], it is essential to include the  $\Delta$  in the intermediate states and evaluate the corresponding contribution to the PV elastic  $ep$  scattering. Similar effect, i.e., TPE contribution with an intermediate  $\Delta$  resonance, in the parity-conserving elastic  $ep$  scattering was found [9] to be small as compared to TPE diagram

with nucleon intermediate states. It can be understood because there is a mismatch in the matrix elements of  $\gamma ee$  and  $\gamma N\Delta$  vertices. Namely, the matrix element of the spatial component of the electron current is  $(v/c)$  smaller than that of the charge component while it is the other way around in the  $\gamma N\Delta$  transition current, i.e., the magnetic dipole transition dominates [10]. However, such a mismatch is absent in the diagrams involving  $Z$ -exchange. We may then expect  $\Delta$  TBE contribution to be non-negligible.

In this paper, we report on calculations of the corrections of the TBE with  $\Delta$  in the intermediate states, including TPE and  $\gamma ZE$ , to  $A_{PV}$  and their effects on the extracted values of the nucleon strange form factors.

At hadron level, the photon-induced transition of  $p \rightarrow \Delta^+$  is given by [9]

$$\begin{aligned} \langle N(p') | J_\mu^{em} | \Delta(p) \rangle &= \frac{F_\Delta(q^2)}{M_N^2} \bar{u}(p') [g_1 (g_\mu^\alpha \not{p} \not{q} - p_\mu \gamma^\alpha \not{q} \\ &- \gamma_\mu \gamma^\alpha p \cdot q + \gamma_\mu \not{p} q^\alpha) + g_2 (p_\mu q^\alpha - p \cdot q g_\mu^\alpha) + g_3 / M_N \\ &(q^2 (p_\mu \gamma^\alpha - g_\mu^\alpha \not{p}) + q_\mu (q^\alpha \not{p} - \gamma^\alpha p \cdot q))] \gamma_5 T_3 u_\alpha^\Delta(p), \end{aligned} \quad (1)$$

where  $q = p' - p$  and  $T_3$  is the third component of the  $N \rightarrow \Delta$  isospin transition operator.

The neutral weak current can be decomposed into isovector and isoscalar parts:

$$\begin{aligned} J_\mu^Z &= \alpha_V V_\mu^3 + \alpha_A A_\mu^3 + \text{isoscalar terms}, \\ J_\mu^{em} &= V_\mu^3 + \text{isoscalar terms}, \end{aligned} \quad (2)$$

where the superscript "3" refers to the 3rd component in isospin space,  $\alpha_V = (1 - 2 \sin^2 \theta_W) / (2 \cos \theta_W)$ , and  $\alpha_A = -1 / (2 \cos \theta_W)$ . The isoscalar part does not contribute to  $N \rightarrow \Delta$  transition. The vector and axial-vector components in the  $Z p \Delta^+$  vertex can be written as

$$\begin{aligned} \langle p(p') | J_\mu^{Z,V} | \Delta^+(p) \rangle &= \frac{F_\Delta(q^2)}{M_N^2} \bar{u}(p') [\tilde{g}_1 (g_\mu^\alpha \not{p} \not{q} - p_\mu \gamma^\alpha \not{q} \\ &- \gamma_\mu \gamma^\alpha p \cdot q + \gamma_\mu \not{p} q^\alpha) + \tilde{g}_2 (p_\mu q^\alpha - p \cdot q g_\mu^\alpha) + \tilde{g}_3 / M_N (q^2 \\ &(p_\mu \gamma^\alpha - g_\mu^\alpha \not{p}) + q_\mu (q^\alpha \not{p} - \gamma^\alpha p \cdot q))] \gamma_5 u_\alpha^\Delta(p), \\ \langle p(p') | J_\mu^{Z,A} | \Delta^+(p) \rangle &= \frac{H_\Delta(q^2)}{M_N^2} \bar{u}(p') [h_1 (g_\mu^\alpha (p \cdot q) - p_\mu q^\alpha) \\ &+ h_2 / M_N^2 (q^\alpha q_\mu \not{p} \not{q} - (p \cdot q) \gamma^\alpha q_\mu \not{p}) + h_3 ((p \cdot q) \gamma^\alpha \gamma_\mu \\ &- \not{p} \gamma_\mu q^\alpha) + h_4 (g_\mu^\alpha p^2 - p_\mu \gamma^\alpha \not{p})] u_\alpha^\Delta(p), \end{aligned} \quad (3)$$

where  $\tilde{g}_i$ 's and  $g_i$ 's are related by  $\tilde{g}_i = \sqrt{2/3} \alpha_V g_i$ .  $F_\Delta$  and  $H_\Delta$  in Eqs. (1) and (3) are vector and axial-vector form factors, respectively, and we assume that, for simplicity, each of them separately take a common form for different couplings.

Choosing the Feynman gauge and neglecting the electron mass  $m_e$  in the numerators, the amplitudes of box diagrams of TBE with  $\Delta$  excitation as depicted in Figs. 2(a) and 2(b) can be written down straightforwardly. E.g., we have for Fig. 2(b)

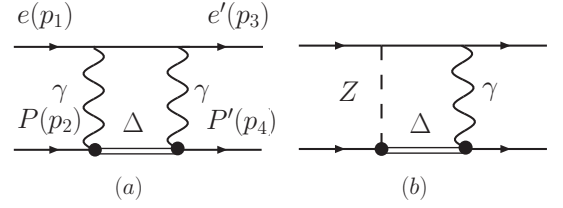


FIG. 2: (a) TPE and (b)  $\gamma ZE$  box diagrams with  $\Delta$  intermediate states. Corresponding crossed diagrams are implied.

$$\begin{aligned} M^{(2b)} &= -i \int \frac{d^4 k}{(2\pi)^4} \bar{u}(p_3) (-ie\gamma_\mu) \frac{i(\not{p}_1 + \not{p}_2 - \not{k})}{(p_1 + p_2 - k)^2 - m_e^2 + i\epsilon} \\ &\times (i \frac{g\gamma_\nu}{4 \cos \theta_W}) [(-1 + 4 \sin^2 \theta_W) + \gamma_5] u(p_1) \frac{-i}{(p_4 - k)^2 + i\epsilon} \\ &\times \frac{-i}{(k - p_2)^2 - M_\Delta^2 + i\epsilon} \bar{u}(p_4) \Gamma_{\Delta \rightarrow N}^{\mu\alpha, \gamma}(k, p_4 - k) \\ &\times \frac{-i(k + M_\Delta) P_{\alpha\beta}^{3/2}(k)}{k^2 - M_\Delta^2 + i\epsilon} \Gamma_{N \rightarrow \Delta}^{\beta\nu, Z}(k, k - p_2) u(p_2), \end{aligned} \quad (4)$$

where  $P_{\alpha\beta}^{3/2}(k)$  [8] is the spin-3/2 projector and  $g = e / \sin \theta_W$  is the weak coupling constant. The vertex functions  $\Gamma$ 's are defined by  $\bar{u}(p') \Gamma_{\Delta \rightarrow N}^{\mu\alpha, \gamma}(p, q) u_\alpha^\Delta(p) = -ie \langle N(p') | J_{em}^{\mu\alpha} | \Delta(p) \rangle$  and  $\bar{u}_\beta^\Delta(p) \Gamma_{N \rightarrow \Delta}^{\beta\nu, Z}(p, -q) u(p') = -ig \langle \Delta(p) | J_Z^{\beta\nu} | N(p') \rangle$ . Note that the vertices  $\gamma N\Delta$  and  $Z N\Delta$  given in Eqs. (1) and (3) both satisfy the constraints,  $p_\alpha \Gamma_{\Delta \rightarrow N}^{\mu\alpha}(p, q') = p_\beta \Gamma_{N \rightarrow \Delta}^{\beta\nu}(p, q') = 0$ , for any  $q'$  to eliminate the coupling of the unphysical spin-1/2 component of Rarita-Schwinger spinor [11].  $Z N\Delta$  vertex has been expressed in several other forms [12, 13, 14] which are different from Eq. (3). All of them, including Eq. (3), are equivalent when both the nucleon and the  $\Delta$  are on-shell. However, only the choice of Eq. (3) contains no coupling to the spin-1/2 component of the  $\Delta$ .

Amplitudes for the cross-box diagrams can be written down similarly. The loop integrals with  $\Delta$  intermediate state are infrared safe. We use computer package "FeynCalc" [15] and "LoopTools" [16] to carry out the calculation. The form factors  $F_\Delta$  and  $H_\Delta$  are necessary for ultraviolet regulation of the loop integral and we assume simple dipole form  $\Lambda_\Delta^4 / (\Lambda_\Delta^2 - q^2)^2$  for both of them. We set  $\Lambda_\Delta = 1$  GeV for  $H_\Delta$  and 0.84 GeV for  $F_\Delta$ . Variations of these cut-offs do not affect significantly the results.

The values of the coupling constants  $g_i$ 's can be determined from the experimental data of  $\gamma N \rightarrow \Delta$  at real photon point. They are simply linear combinations of the Jones-Scadron form factors [17]  $G_{(M,E,C)}$  at  $Q^2 = 0$ ,

$$\begin{aligned} g_1 &= K (G_E(0) - G_M(0)), \\ g_2 &= K \left( -\frac{M_\Delta + 3M_N}{M_\Delta - M_N} G_E(0) - G_M(0) \right), \\ g_3 &= \frac{KM_N}{M_\Delta} \left( -\frac{(M_\Delta + M_N)G_C(0)}{M_\Delta - M_N} + \frac{4M_\Delta^2 G_E(0)}{(M_\Delta - M_N)^2} \right), \end{aligned}$$

where  $K = \frac{3}{2} \frac{M_N}{M_\Delta + M_N}$ . With the use of the most recent experimental values for the  $G's(0)$  [8, 18], we obtain  $g_1 = 1.91$ ,  $g_2 = 2.63$ , and  $g_3 = 1.59$ . These give  $\tilde{g}_1 = 0.48$ ,  $\tilde{g}_2 = 0.66$ , and  $\tilde{g}_3 = 0.40$ . They differ from those used in [9] where  $G_C(0)$  was approximated to be zero.

Only coupling constants  $h_i's$  remain to be determined. They can be inferred from the data of  $\nu N \rightarrow \mu \Delta$ . Many experimental papers on neutrino induced  $\Delta$  production adopt the notation of Llewellyn-Smith [12] where the  $N$ - $\Delta$  transition is written as

$$\begin{aligned} \langle \Delta^{++}(p') | J_\mu^W | p(p) \rangle = & \bar{u}_\alpha(p') \left[ \left( \frac{C_3^V}{M_N} \gamma^\lambda + \frac{C_4^V}{M_N^2} p'^\lambda + \right. \right. \\ & \left. \left. \frac{C_5^V}{M_N^2} p^\lambda \right) (q_\lambda g_\mu^\alpha - q_\mu g_\lambda^\alpha) \gamma_5 + C_6^V g_\mu^\alpha \gamma_5 + \left( \frac{C_3^A}{M_N} \gamma^\lambda + \right. \right. \\ & \left. \left. \frac{C_4^A}{M_N^2} p'^\lambda \right) (q_\lambda g_\mu^\alpha - q_\mu g_\lambda^\alpha) + C_5^A g_\mu^\alpha + \frac{C_6^A}{M_N^2} p^\alpha q_\mu \right] u(p). \end{aligned} \quad (5)$$

The form factors in Eq. (3) can be related to the form factors defined in Eq. (5) by performing a rotation in isospace and assuming the nucleon and  $\Delta$  are both on-shell. The resulting relations are

$$\begin{aligned} h_1 &= -\frac{\beta C_4^A(0)}{\sqrt{3}} + \frac{2M_N}{M_\Delta} \frac{\beta C_3^A(0)}{\sqrt{3}}, \\ h_3 &= -\frac{M_N}{M_\Delta} \cdot \frac{\beta C_3^A(0)}{\sqrt{3}}, \quad h_2 = \frac{M_N^2}{M_\Delta(M_\Delta - M_N)} \frac{\beta C_6^A(0)}{\sqrt{3}}, \\ h_4 &= -\frac{M_N^2}{M_\Delta^2} \frac{\beta C_5^A(0)}{\sqrt{3}} - \frac{M_N(M_\Delta - M_N)}{M_\Delta^2} \frac{\beta C_3^A(0)}{\sqrt{3}}. \end{aligned} \quad (6)$$

According to [19, 20]  $C_3^A=0$ , hence  $h_3=0$ . From the data of  $\nu N \rightarrow \mu N \pi$  [21] one can extrapolate the experimental result to  $Q^2=0$  and find  $C_4^A(0) = -0.8$  and  $C_5^A(0) = 2.4$  [13]. One then obtains  $h_1 = -0.263$ , and  $h_4 = -0.458$ . Parameter  $h_2$  can not be determined from the weak pion production. Fortunately its effect is tiny ( $\leq 10^{-18}$ ) and we simply set  $h_2 = 0$ . The sensitivity of the results with respect to the variation of  $h_i's$  is found to be very small.

In Fig. 3, we show the TPE and  $\gamma ZE$  corrections to  $A_{PV}$  by plotting  $\delta = \delta_N + \delta_\Delta$ , defined by

$$A_{PV}(1\gamma + Z + 2\gamma + \gamma Z) = A_{PV}(1\gamma + Z)(1 + \delta_N + \delta_\Delta), \quad (7)$$

vs.  $\epsilon \equiv [1 + 2(1 + \tau) \tan^2 \theta_{Lab}/2]^{-1}$ , where  $\theta_{Lab}$  is the laboratory scattering angle and  $\tau = Q^2/(4M^2)$ , at four different values of  $Q^2 = 0.1, 0.5, 1.0, \text{ and } 3.0 \text{ GeV}^2$ .  $A_{PV}(1\gamma + Z)$  denotes the parity-violating asymmetry arising from the interference between OPE and  $Z$ -boson-exchange, i.e., Figs. 1(a) and 1(b), while  $A_{PV}(1\gamma + Z + 2\gamma + \gamma Z)$  includes the effects of TPE and  $\gamma ZE$ .  $\delta_N$  and  $\delta_\Delta$  correspond to the contribution from the box diagrams with only nucleon or  $\Delta$  in the intermediate states and are represented by dotted and dot-dashed lines, respectively. The sum  $\delta = \delta_N + \delta_\Delta$  is given by solid curves. In addition, we also present the contribution arising from interference

between  $\gamma ZE$  with  $\Delta$ -excitation and OPE,  $\delta_\Delta(\gamma Z)$  by short dashed lines. The difference between dot-dashed lines and short dashed lines would then correspond to effects of interference between TPE with  $\Delta$ -excitation and  $ZBE$ , i.e.,  $\delta_\Delta(2\gamma) = \delta_\Delta - \delta_\Delta(\gamma Z)$ .

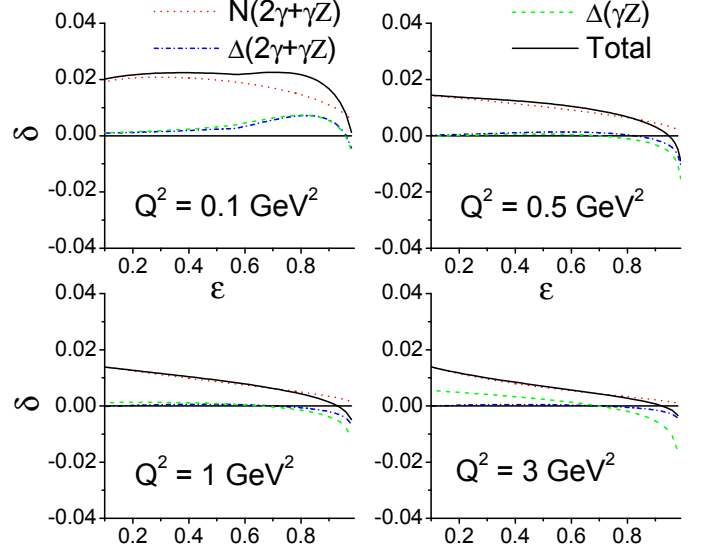


FIG. 3: TPE and  $\gamma Z$ -exchange corrections with nucleon and  $\Delta$  intermediate states to parity-violating asymmetry as functions of  $\epsilon$  from 0.1 to 0.98 at  $Q^2 = 0.1, 0.5, 1.0, \text{ and } 3.0 \text{ GeV}^2$ .

We see from Fig. 3, that  $\delta_\Delta$  (dot-dashed lines) is very small except at low  $Q^2 \sim 0.1 \text{ GeV}^2$  and  $\epsilon \geq 0.7$ . Detailed analysis shows that below  $Q^2 \sim 0.1 \text{ GeV}^2$ ,  $\delta_\Delta(\gamma Z)$  starts out as very small and positive at small  $\epsilon$  and increases with  $\epsilon$  before turning around at  $\epsilon \sim 0.9$  and drops sharply to become large and negative as  $\epsilon$  approaches 1. The peak around  $\epsilon \sim 0.9$  is very sharp and becomes less pronounced with increasing  $Q^2$ . In this region of small  $Q^2$ ,  $\delta_\Delta(2\gamma)$  is almost negligible. For  $Q^2$  in the region of  $0.1 \sim 1.0 \text{ GeV}^2$ , both  $\delta_\Delta(2\gamma)$  and  $\delta_\Delta(\gamma Z)$  are flat and almost zero until  $\epsilon$  increases past 0.8 and results in a small and negative  $\delta_\Delta$  at forward angles. For  $Q^2 \geq 3.0 \text{ GeV}^2$ ,  $\delta_\Delta(\gamma Z)$  starts out around 1% at backward angles and gradually decreases with increasing  $\epsilon$  to cross zero at  $\epsilon \sim 0.7$  before dipping further to large and negative at extreme forward angles. However, the total effects of the  $\Delta$ ,  $\delta_\Delta$  is small at  $Q^2 \geq 1.0 \text{ GeV}^2$ . These behaviors differ from those of  $\delta_N$  which always stays positive and decreases with increasing  $\epsilon$ . At small  $\epsilon$ ,  $\delta_N$  is much greater than  $\delta_\Delta$  such that the sum  $\delta$  is not much different from  $\delta_N$ . However, for larger values of  $\epsilon$ ,  $\delta_\Delta$  dominates.

Another way to look at our results is to see the evolution of the  $\delta's$  with respect to  $Q^2$  at fixed  $\epsilon$  as depicted in Fig. 4 for  $\epsilon = 0.5$  and  $\epsilon = 0.95$ . The notation is the same as in Fig. 3. We clearly see that at  $\epsilon = 0.5$ ,  $\delta_N$  is dominant. However, at  $\epsilon \geq 0.95$  where most of the existing data are taken,  $\delta_\Delta$  dominates.

We now proceed to estimate the effects of the TBE

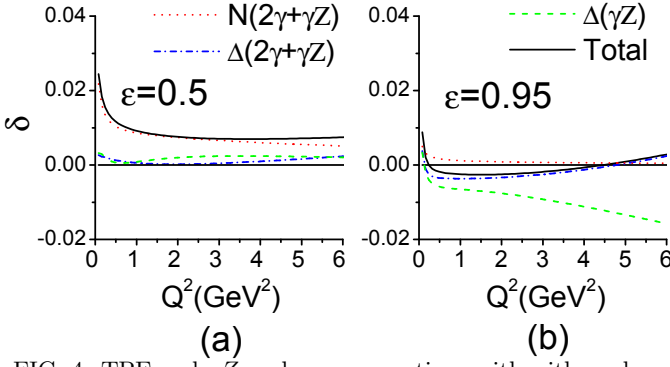


FIG. 4: TPE and  $\gamma Z$ -exchange corrections with nucleon and  $\Delta$  intermediate states to parity-violating asymmetry as functions of  $Q^2$  from 0.1 to 6  $\text{GeV}^2$  at  $\epsilon = 0.5$  and 0.95.

on the values of strange form factors extracted from HAPPEX, A4 and G0 [1] experiments. The parity asymmetry is conveniently [4] expressed as follows,

$$\begin{aligned}
 A_{PV}(\rho, \kappa) &= A_1 + A_2 + A_3, \\
 A_1 &= -a\rho \left[ (1 - 4\kappa \sin^2 \theta_W) - \frac{\epsilon G_E^{\gamma,p} G_E^{\gamma,n} + \tau G_M^{\gamma,p} G_M^{\gamma,n}}{\epsilon (G_E^{\gamma,p})^2 + \tau (G_M^{\gamma,p})^2} \right], \\
 A_2 &= a\rho \frac{\epsilon G_E^{\gamma,p} G_E^s + \tau G_M^{\gamma,p} G_M^s}{\epsilon (G_E^{\gamma,p})^2 + \tau (G_M^{\gamma,p})^2}, \\
 A_3 &= a(1 - 4 \sin^2 \theta_W) \frac{\epsilon' G_M^{\gamma,p} G_A^Z}{\epsilon (G_E^{\gamma,p})^2 + \tau (G_M^{\gamma,p})^2}, \quad (8)
 \end{aligned}$$

where  $a = G_F Q^2 / 4\pi\alpha\sqrt{2}$ ,  $\epsilon' = \sqrt{\tau(1+\tau)(1-\epsilon^2)}$ , and  $\alpha$  the fine structure constant. When the parameters  $\rho$  and  $\kappa$  are set to one, Eq. (8) reduces to the expression obtained in tree approximation. The linear combination of the strange form factors  $G_E^s + \beta G_M^s$ , with  $\beta = \tau G_M^{\gamma,p} / \epsilon G_E^{\gamma,p}$  has been extracted from  $A_2$  in Eq. (8). Deviations of  $\rho$  and  $\kappa$  from one represent all possible higher-order radiative corrections, including vertex corrections, corrections to the propagators, and  $\gamma Z$ -exchange etc.

The latest PDG values [22] give  $\rho = 0.9876$ ,  $\kappa = 1.0026$ . To avoid double counting, one should remove the effect of the  $\gamma Z$  box diagram. The values  $\delta\rho = -3.7 \times 10^{-3}$  and  $\Delta\kappa = -5.3 \times 10^{-3}$  for this effect used in PDG were those estimated by [3] within the zero momentum transfer  $Q \equiv 0$  approximation scheme, when the onset scale is set to be 1 GeV. Consequently, we will set the experimental parity asymmetry,

$$\begin{aligned}
 A_{PV}^{(Exp)} &\equiv A_{PV}(1\gamma + Z + 2\gamma + \gamma Z), \\
 &= A_{PV}(\rho', \kappa')(1 + \delta_N + \delta_\Delta). \quad (9)
 \end{aligned}$$

where  $\rho' = \rho - \Delta\rho$  and  $\kappa' = \kappa - \Delta\kappa$ . We can then determine  $A_{PV}(\rho', \kappa')$  and extract the strange form factors from the resultant  $A_2$ .

We introduce  $\delta_G$

$$\overline{G}_E^s + \beta \overline{G}_M^s = (G_E^s + \beta G_M^s)(1 + \delta_G), \quad (10)$$

to quantify the effects of TBE, where  $G_E^s + \beta G_M^s$  and  $\overline{G}_E^s + \beta \overline{G}_M^s$  correspond to the strange form factors extracted from  $A_{PV}(\rho, \kappa)$  and  $A_{PV}(\rho', \kappa')$ , respectively. From Eq. (8) we then obtain

$$\delta_G = \frac{A_{PV}^{Exp} \left( \frac{\Delta\rho}{\rho} - \delta \right) + 4a\rho \sin^2 \theta_W \Delta\kappa - A_3 \frac{\Delta\rho}{\rho}}{A_{PV}^{Exp} - A_0}, \quad (11)$$

where  $A_0 = A_1 + A_3$ .

We present our results for  $\delta_N$ ,  $\delta_\Delta$ , their sum  $\delta$ , and  $\delta_G$  in Table I for HAPPEX, A4, and G0 experiments. We also list the corresponding values, labelled as  $\delta_0$ , in Table I as would be obtained in [3] within  $Q \equiv 0$  approximation scheme such that  $\delta_G = 0$  if  $\delta = \delta_0$ . In other words, difference between  $\delta$  as we obtain and  $\delta_0$  represents the possible  $Q^2$ -dependence neglected in the estimation of [3].

	I	II	III	IV	V	VI
$Q^2(\text{GeV}^2)$	0.477	0.109	0.23	0.108	0.232	0.410
$\epsilon$	0.974	0.994	0.83	0.83	0.986	0.974
$\delta_N(\%)$	0.25	0.34	0.86	1.30	0.288	0.275
$\delta_\Delta(\%)$	-0.59	-1.53	0.21	0.66	-0.90	-0.60
$\delta(\%)$	-0.34	-1.19	1.07	1.96	-0.61	-0.30
$\delta_0(\%)$	1.03	2.62	1.51	3.13	1.82	1.417
$\delta_G(\%)$	-25.52	-75.23	-2.76	-2.27	13.12	20.62

TABLE I: The corrections  $\delta_G$  to  $G_E^s + \beta G_M^s$  for HAPPEX, A4, and G0 experiments. (I, II), (III, IV), and (V, VI) refer to the HAPPEX, A4, and G0 data, respectively [1].

All experimental data included in Table I were obtained in near forward directions with  $\epsilon \geq 0.8$ . More specifically, the HAPPEX and G0 data given in the columns (I, II) and (V, VI) were taken at extremely forward angles with  $\epsilon \approx 0.97$ . It is seen that in this region  $\delta_\Delta$  completely dominates over  $\delta_N$  with opposite sign and pushes the total TBE effects  $\delta = \delta_N + \delta_\Delta$  away from the zero momentum transfer approximation values  $\delta_0$ . Thus the large corrections to  $\delta_G$  we found in [5] for HAPPEX data in columns (I, II) with only effect of nucleon intermediate states considered, are now enhanced from  $(-14.6\%, -45.1\%)$  to  $(-25.5\%, -75.2\%)$ , respectively. Similarly, for the case of G0 data given in (V, VI),  $\delta_G$  increases from  $(7.7\%, 13.6\%)$  to  $(13.1\%, 20.6\%)$ , respectively. However, for A4 data listed in columns (III, IV) taken at smaller  $\epsilon = 0.83$ ,  $\delta_\Delta$  is smaller than  $\delta_N$  with same sign such that  $\delta_\Delta$  brings  $\delta$  close to  $\delta_0$  and results in smaller  $\delta_G$ 's.

In summary, we calculate TBE effect with  $\Delta$  excitation to the parity-violating asymmetry of elastic  $ep$  scattering in a simple hadronic model.  $\Delta$ 's contribution  $\delta_\Delta$  is, in general, much smaller compared with the nucleon contribution  $\delta_N$  in magnitude except at extreme forward angles.  $\delta_\Delta$  stays very small and flat at backward angles but turn negative and large at extreme forward angles, in

contrast to  $\delta_N$  which always stays positive but decreases monotonically with increasing  $\epsilon$ . Accordingly, interplay between the contributions of TBE with nucleon and  $\Delta$  intermediate states depends strongly on the kinematics. The  $\Delta$  effect is smaller in magnitude than the nucleon contribution with the same sign for  $\epsilon \leq 0.8$ , as in the case of A4 experiments. The total TBE effect  $\delta = \delta_N + \delta_\Delta$  is hence enhanced and approaches closer to the zero momentum transfer approximation value  $\delta_0$  than  $\delta_N$ . Thus the corrections to  $G_E^s + \beta G_M^s$  in A4 experiments decrease to about  $-2.5\%$ , when the effect of  $\Delta$  excitation is included. On the other hand, at extremely forward directions with  $\epsilon \sim 0.97$ , as in the cases of HAPPEX and G0 experiments,  $\Delta$ 's effect becomes negative and dominates over  $\delta_N$ . The sum  $\delta$  then moves considerably away from  $\delta_0$ . The combined TBE correction to  $G_E^s + \beta G_M^s$  found in [5] for the HAPPEX experiments are thereby enhanced to reach  $-25\% \sim -75\%$ , while in the case of G0 experiments the corrections are in the range of  $13\% \sim 21\%$ .

The fact that we find significant contribution from TBE with  $\Delta$  excitation in the very forward angles, where many of the current experiments are performed, brings up the question of the inclusion of higher resonances. Naively, one would expect that  $\Delta(1232)$  would give the largest contribution since it is the most prominent resonance and, besides, higher resonances are suppressed because of their larger masses. However, only an explicit microscopic calculation can answer this question. An extension of the present calculation to include higher resonances is currently underway. Recent dispersion relation calculation of the  $\gamma ZE$  correction to  $Q_{weak}$  [23] could be used to clarify this question in the exact forward scattering. However, our results indicate that  $\delta$  depends sensitively with  $Q^2$  at low momentum transfer so whether dispersion relation method of [23] can be extended to investigate the TBE correction to strange form factors remains to be further explored. Study of TBE effect with the use of GPD as done in [7] and [24] for TPE effects, will also be very illuminating in this regard.

We thanks P.G. Blunden for helpful discussions regarding the numerical part of this calculation. This work is supported by the National Science Council of Taiwan under grants nos. NSC096-2112-M033-003-MY3 (K.N and C.W.K.) and NSC096-2112-M022-021 (S.N.Y.) and by National Natural Science Foundation of China under grant nos 1974118 and 10805009 (H.Q.Z). H.Q.Z. gladly acknowledges the support of NCTS/North of Taiwan for his visit and the warm hospitality extended to him by National Taiwan University. K.N. also acknowl-

edges the support of NCTS/HsinChu of Taiwan for his visit to Manitoba.

- 
- [1] D.T. Spayde *et al.* (SAMPLE), Phys. Lett. **B 583**, 79 (2004); A. Acha *et al.* (HAPPEX), Phys. Rev. Lett. **98**, 032301 (2007); B. Glaser (for the A4 collaboration) Eur. Phys. J. **A 24**, **S2**, 141 (2005); C. Furget (for the G0 collaboration), Nucl. Phys. Proc. Suppl. **159**, 121 (2006); and references contained therein.
  - [2] D. Kaplan, A. Manohar, Nucl. Phys. **B 310**, 527 (1988).
  - [3] W.J. Marciano and A. Sirlin, Phys. Rev. **D 27**, 552 (1983); *ibid.* **D 29**, 75 (1984).
  - [4] M.J. Musolf and B.R. Holstein, Phys. Lett. **B 242**, 461 (1990); M.J. Musolf, *et al.*, Phys. Rept. **239**, 1 (1994); J. Erler, A. Kurylov, and M.J. Ramsey-Musolf, Phys. Rev. **D 68**, 016006 (2003).
  - [5] H.Q. Zhou, C.-W. Kao and S.N. Yang, Phys. Rev. Lett. **99**, 262001 (2007); *ibid.* **100**, 059903(E) (2008).
  - [6] J.A. Tjon and W. Melnitchouk, Phys. Rev. Lett. **100**, 082003 (2008).
  - [7] A.V. Afanasev, C.E. Carlson, Phys. Rev. Lett. **94**, 212301 (2005).
  - [8] V. Pascalutsa, M. Vanderhaeghen, and S.N. Yang, Phys. Rept. **437**, 125 (2007).
  - [9] S. Kondratyuk, P.G. Blunden, W. Melnitchouk and J.A. Tjon, Phys. Rev. Lett. **95**, 172503 (2005).
  - [10] S.S. Kamalov and S.N. Yang, Phys. Rev. Lett. **83**, 4494 (1999).
  - [11] V. Pascalutsa and R. Timmermans, Phys. Rev. **C 60**, 042201 (1999).
  - [12] C.H. Llewellyn Smith, Phys. Rept. **3**, 261 (1972).
  - [13] T. R. Hemmert, B. R. Holstein and N.C. Mukhopadhyay, Phys. Rev. **D 51**, 158 (1995).
  - [14] L. M. Nath, K. Schilcher and M. Kretzschmar, Phys. Rev. **C 25**, 2300 (1982).
  - [15] R. Mertig, M. Bohm, and A. Denner, Comput. Phys. Commun. **64**, 345 (1991).
  - [16] T. Hahn, M. Perez-Victoria, Comput. Phys. Commun. **118**, 153 (1999).
  - [17] H.F. Jones and M.D. Scadron, Ann. Phys. **81**, 1 (1973)
  - [18] D. Drechsel, S.S. Kamalov, and L. Tiator, Eur. Phys. J. **A 34**, 69 (2007).
  - [19] S. L. Adler, Ann. of Phys. **50**, 189 (1968).
  - [20] P.A. Schreiner and F.V. Hippel, Nucl. Phys. **B58**, 333 (1973).
  - [21] T. Kitagaki *et al.*, Phys. Rev. **D 42**, 1331 (1990).
  - [22] C. Amslet *et al.*, Phys. Lett. **B 667**, 1 (2008).
  - [23] M. Gorchtein and C.J. Horowitz, Phys. Rev. Lett. **102**, 091806 (2009).
  - [24] Y.C. Chen, A.V. Afanasev, S.J. Brodsky, C.E. Carlson, and M. Vanderhaeghen, Phys. Rev. Lett. **93**, 122301 (2004).